Scientific Research Publishing

Open Journal of Optimization, 2025, 14(3), 111-130
https://www.scirp.org/journal/ojop
ISSN Online: 2325-7091
ISSN Print: 2325-7105

A Response Surface Methodology Approach for Improving OMUX Resonator Quality Factor

Khaled Khoder[1], Annie Bessaudou[2], Françoise Cosset[2], Christophe Durousseau[2]

[1]Capgemini Engineering, Toulouse, France
[2]Xlim Research Institute UMR CNRS 7252, Limoges, France
Email: khaled.khoder@capgemini.com

How to cite this paper: Khoder, K., Bessaudou, A., Cosset, F. and Durousseau, C. (2025) A Response Surface Methodology Approach for Improving OMUX Resonator Quality Factor. *Open Journal of Optimization*, **14**, 111-130.
https://doi.org/10.4236/ojop.2025.143007

Received: April 21, 2025
Accepted: July 27, 2025
Published: July 30, 2025

Copyright © 2025 by author(s) and Scientific Research Publishing Inc.
This work is licensed under the Creative Commons Attribution International License (CC BY 4.0).
http://creativecommons.org/licenses/by/4.0/

Open Access

Abstract

In this paper, the successful use of Response Surface Methodology (RSM) in optimizing the characteristics of an OMUX resonator is presented. Models for the output responses, with respect to geometric design parameters, are developed using Design of Experiments (DOE) based RSM and Finite Element Method (FEM) simulations. A single optimization objective function, considering all the output responses, is defined and optimized for the design factors. RSM is then coupled with Level Set (LS) method to maximize the quality factor of the OMUX resonator. The proposed optimization process resulted in a 25.3 % improvement in the quality factor compared to the reference value. Moreover, coupling these two optimization methods leads to a structure presenting a volume 34.5% lower than that identified by using RSM only.

Keywords

Multicriteria Optimization, Central Composite Designs, Response Surface Methodology, OMUX Filters, Level Set, Desirability Functions

1. Introduction

Response surface methodology (RSM) was initially developed and described by Box and Wilson (1951) [1]. They are developed in different scientific fields, in particular: biology, chemistry, human sciences and agronomy [2]-[4].

RSM consists of a group of mathematical and statistical techniques used in the development of an adequate functional relationship between a response of interest, y, and a number of associated control (or input) variables denoted by x_1, x_2, ..., x_k.

Generally, one factor or process variable can depend on or be dependent on another variable in an experimental design. Knowledge of the interaction between

the factors is crucial in finding the output-input relationship. This is why relationships are hardly determined using a one-factor-at-a-time method. By establishing a model equation, RSM can evaluate the relationship as well as interactions among the multiple parameters using quantitative data.

The objective of this methodology is, more than to prioritize the effects of the different input factors, to describe as precisely as possible the behavior of the response according to the variations of the factors. The aim of this type of study is therefore to reach a model of the studied phenomenon based on experimentation. These designs allow for the determination of the values at which the input factors of a device must be adjusted to obtain one or several desired responses; they are based on the use of models of a polynomial nature.

The number of experiments in an RSM design increases rapidly with the number of factors. For experiments to be designed effectively and economically, the number of factors used should be limited. For this reason, screening designs are used to screen a large number of process or design parameters to identify the most important parameters that will have a significant impact on the process performance. Once the key parameters are identified, RSM designs are used [5] [6].

In this paper, RSM is applied to optimize the characteristic of an OMUX resonator [7]; Central composite design (CCD), as the most popular form of RSM used in the process of optimization studies, is used extensively in building the second-order response surface models [8] [9]. First, a brief review of RSM and CCD is presented, as well as mathematical model validation and multicriteria optimization steps. In a second section, RSM is applied to optimize the dimensions of the cylindrical cavity containing the OMUX resonator; in this case, only two input factors are considered using two CCDs designs in the spherical and cubic domains. The last section deals with the coupling between RSM and Level Set (LS) method to optimize the OMUX resonator while trying to decrease the cavity dimensions. Finally, the optimized resonator is fabricated and an improvement on the quality factor by 25.77% is obtained.

2. Review on Response Surface Methodology

RSM has been developed in order to optimize a response variable by adjusting the values of factors when the functional relationship among the variables is unknown. It relies on the use of models such as a polynomial. The more the degree of the model, the closer we approach the phenomenon observed, but the number of experiments becomes more important. This leads us to adopt a compromise: we consider a polynomial model of degree 2, which is written as follows:

$$\hat{Y} = b_0 + \sum_{i=1}^{k} b_i X_i + \sum_{i=1}^{k} b_{ii} X_i^2 + \sum_{i=1}^{k-1} \sum_{j=i+1}^{k} b_{ij} X_i X_j + \varepsilon \quad (1)$$

In this expression, $\hat{Y}$ represents the predicted response; b_0, b_i and b_{ij} are the coefficients to estimate; X_i and X_j are the coded values of the variable parameters (input factors); and ε is the random error. The number of coefficients of second-degree model is given by the following formula:

$$p = \frac{(k+2)!}{k!2!} \tag{2}$$

In most cases, the input factors reflect different sizes and/or are expressed in different units. It is therefore necessary to standardize the changes of these variables to make them comparable with no units. This is a relationship of coding (centering and reduction) factor, given by formula:

$$X_i = \frac{u_i - \left(\frac{u_{\max} + u_{\min}}{2}\right)}{\left(\frac{u_{\max} - u_{\min}}{2}\right)} \tag{3}$$

$u_{\min}$ and $u_{\max}$ represent the limits of the factor that are specified by the user. After recoding using (3), the factor's coded values are used through the matrix of experiments in order to get the experiment design. More than prioritizing the effects of different factors, the objective of this methodology is to describe the behavior of the response as precisely as possible. Different types of experimental designs using the response surfaces methodology have already been studied [10]. Choosing a design requires an understanding of the factors studied and knowledge of the type of experiment. In the case of a long-term experiment, we must be interested in economic designs that have a low number of experiments. In cases where experiments are less time-consuming, we are interested in greedy designs in terms of the number of experiments, but more accurate in terms of results. Among the many types of response surface designs, we present here only the most conventionally used: Central Composite Designs (CCDs).

2.1. Central Composite Designs

CCDs employ the methodology of response surfaces; their construction consists of adding points (star points) to a full factorial design [11]. However, they are very greedy in terms of the number of experiments compared to other types of designs but it is conceivable when the number of factors studied is low (between 2 and 4). The number of experiments in a central composite design is given by the following equation:

$$N = 2^k + 2k + n_0 \tag{4}$$

where k is the number of factors. A central composite design is the sum of three terms:

- a full factorial design (2k experiments);
- two-star points by a factor that are positioned on the axis of each of them to a distance α from the center. These points contribute to the evaluation of quadratic terms in the polynomial model;
- n_0 repetitions at the center of experimental field, dedicated to statistical analysis. In cases of numerical simulations, the number of repetitions at the center of experimental field is equal to 1 (no experimental error).

The three components, namely axial distance, factorial points, and the number of center runs, play important and somewhat different roles. The factorial points contribute to the estimation of linear terms and two-factor interactions. The axial points contribute in a large way to estimation of pure quadratic terms. Axial distance greatly depends on the region of operability and region of interest while the rotatability, robustness of extrapolation, estimation precision of parameters, and location of optimized points all reside in the selection of α. The center runs provide an internal estimate of error (pure error) and estimation of uniform precision. Significant differences in centre points play an important and different role in different designs of interest.

Central composite designs can be used in two domains: spherical and cubic. In the first case, two designs are used: the Circumscribed Central Composite (CCC) and the Central Composite Inscribed (CCI), in the second case, it's called Central Composite Face centered (CCF).

2.1.1. Circumscribed Central Composite (CCC)

In this type of design, each factor takes 5 levels and the experimental field is spherical. In this case, if $k = 2$ factors, the experimental field is within a circle of radius α. The two axes represent the variation of two coded factors X_1 and X_2. Coded values of each factor are given in the experiment's matrix reported in **Table 1**.

The first four experiments represent the full factorial design (possible combinations of −1 and +1 levels of each factor). Experiments 5 to 8 represent the star points; each factor has its largest value in the design. It is shown that for two factors, and to maintain rotatability, the value of α depends on the number of experimental runs in the factorial portion of the central composite design [12]-[15]:

$$\alpha = \sqrt[4]{2^k} \tag{5}$$

The last point of the matrix represents the center of the domain (0, 0). After building the experiments matrix with coded values, the next step consists of building the design of experiments using relation (3).

2.1.2. Circumscribed Central Inscribed (CCI)

The experimental domain occupied by a CCI design is a spherical domain, the value of α is equal to 1, and the extreme coded values are then −1 and 1. This design is composed of a point at the center of the domain (0, 0), the vertices of the domain which are combinations between the levels $-a$ and a of each factor and star points which are located at a unit distance from the center of the domain.

The CCI designs have the same functionality as the CCC designs described above. The advantage here comes from the fact that the extreme values of the coded factors are −1 and +1, which facilitates the transition from the matrix of experiments to the design of experiments. The value of a is given by:

$$a = \frac{\sqrt{k}}{k} \tag{6}$$

In the case of two factors, a is equal to 0.7071, the vertices of the design corre-

spond to the first four experiments in the matrix as shown in Table 1, experiments 5 to 8 represent the star points, considering a single point in the center of the domain (experiment 9).

2.1.3. Central Composite Face-Centered (CCF)

In this type of design, the experimental domain is a cubic domain; each factor requires 3 levels, which are −1, 0, and 1. These designs are used in the case where no operating point of the device is known, the experimental domain is limited by a square, which gives the possibility to find the optima that are next to the extreme values of the factors (which is not possible in a spherical domain). The value of α is equal to 1; the vertices of the domain are combinations with the values −1 and 1 of the input factors, which explains the number of levels of each factor, which is limited to 3.

The matrix of experiments for a CCF design also consists of 3 parts as shown in Table 1.

Table 1. Coded variable data for CCC, CCI and CCF designs for two factors.

Central Composite Designs	Experiment number	CCC		CCI		CCF	
		X_1	X_2	X_1	X_2	X_1	X_2
Full Factorial design	1	−1	−1	$-a$	$-a$	−1	−1
	2	1	−1	a	$-a$	1	−1
	3	−1	1	$-a$	a	−1	1
	4	1	1	a	a	1	1
Star points	5	1	0	1	0	1	0
	6	−1	0	−1	0	−1	0
	7	0	α	0	1	0	1
	8	0	−1	0	−1	0	−1
Center point	9	0	0	0	0	0	0

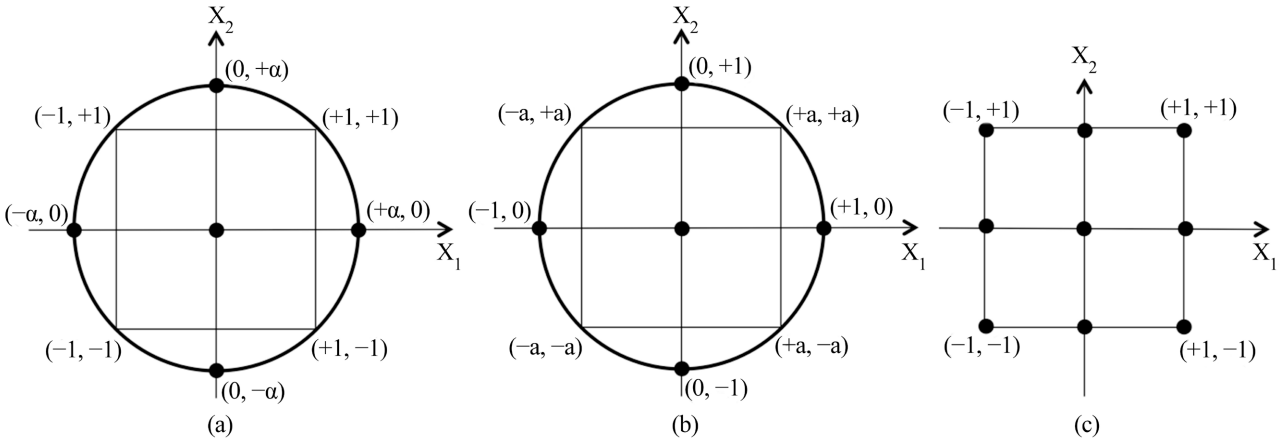

Figure 1. Different types of Central Composite Designs: (a) CCC; (b) CCI; (c) CCF.

The use of a design in a spherical area is recommended since each factor requires five levels, which gives high accuracy for the mathematical models. A spherical field is generally used whenever we know an operating point of the device to optimize; this is usually the center of the spherical field. When the location of the optimum is totally unknown, a design in a cubic field is recommended. The optimum can be found for extreme levels of factors. Figure 1 shows the graphical representation of the three types of CCDs for two input factors.

2.2. Evaluation of the Model Quality

To define the quality of models for each response, the ANalysis of VAriance (ANOVA) is studied; for this, several terms must be defined [16] [17]:

SCT is the sum of squares, that is the sum of squared deviations between the results of simulations (Y_i) and the average ($\overline{Y}$); it is given by:

$$SCT = \sum_{i=1}^{N} \left(Y_i - \overline{Y} \right)^2 \tag{7}$$

The total sum of squares (*SCT*) can be given by the following equation, also called the equation of analysis of variance or regression equation:

$$SCT = SCM + SCE \tag{8}$$

The first term reflects the variation of responses calculated by the model ($\hat{Y}_i$) around the mean value, given by:

$$SCM = \sum_{i=1}^{N} \left(\hat{Y}_i - \overline{Y} \right)^2 \tag{9}$$

The second term reflects the sum of square of the residuals:

$$SCE = \sum_{i=1}^{N} \left(Y_i - \hat{Y}_i \right)^2 \tag{10}$$

A statistical test to reject the hypothesis (H_0) that the model does not describe the variation of the experiments will then be defined. When this hypothesis is verified, it can be shown that the statistic F_c follows respectively $(p-1)$ and $(N-p)$ degrees of freedom with p the number of coefficients to be estimated and N the number of experiments:

$$F_c = \frac{SCM\left(p-1\right)}{SCE\left(N-p\right)} \tag{11}$$

Thus, the hypothesis (H_0) is rejected with probability α if:

$$F_c > F_{(\alpha, p-1, N-p)} \tag{12}$$

In this equation, $F_{(\alpha, p-1, N-p)}$ is the $(1-\alpha)$ quantile of a Fisher's law with $(p-1)$ and $(N-p)$ degrees of freedom.

The model can describe the variation of the experimental results if the probability of rejecting the null hypothesis is low (Prob (F_c) < 5%).

All these data lead to the construction of the ANOVA table, summarizing the different results as shown in Table 2. ANOVA table could be used to calculate the coefficient of determination R^2 from the following equation:

$$R^2 = \frac{SCM}{SCT} = 1 - \frac{SCE}{SCT} \tag{13}$$

This coefficient reflects the model's contribution to the observed response variation. The R^2 value is always between 0 and 1. Values close to 1 indicate a very good model.

In the presence of several explicative variables, which is usually the case, it is imperative to avoid using the coefficient of determination R^2 to estimate the descriptive quality of the model. The adjusted coefficient of determination is used; it is given by the following formula:

$$R^2_{adj} = 1 - \frac{N-p}{SCT} \tag{14}$$

Another coefficient to describe the predictive ability of the model, called R^2_{pred} is given by the formula:

$$R^2_{pred} = 1 - \frac{PRESS}{SCT} \tag{15}$$

where PRESS (Prediction Residual Error Sum of Square), the sum of squared residuals, is given by the following formula:

$$PRESS = \sum_{i=1}^{N} e(i)^2 \tag{16}$$

The regression has been done without the experience i and for each $(N-1)$ points we calculate $\hat{Y}_i$ at point i: $e(i) = Y_i - \hat{Y}_i$, the procedure has been repeated for each point ($i = 1, 2, \cdots, N$) where $\hat{Y}_i$ is the value of the response calculated by model and Y_i the value of the response obtained by simulation at point i. The value of R^2_{pred} ranges between 0 and 1. Large R^2_{pred} (>0.7) indicates that the model has good predictive ability and will have small prediction errors.

Table 2. Analysis of variance (ANOVA) table.

Source	Sum of squares	Degree of freedom	Mean square	F_c
Regression	SCM	$P-1$	A = $SCM/p-1$	A/B
Error	SCE	$N-p$	B = $SCE/N-p$	
Total	SCT	$N-1$		

2.3. Multicriteria Optimization: Desirability Functions

When there are several responses to be optimized, the notion of desirability will be used. This concept was introduced by E.C. Harrington [18] in 1965, and was later developed, notably by G. Derringer [19]. It is based on the transformation of all responses obtained from different measurement scales into an identical dimensionless desirability scale (individual desirability). The values of the individual desirability functions (d_i) are between 0 and 1. Then, the set of individual desirabilities is gathered into a single global desirability D [20], which is their geometric

mean. The particularity of the geometric mean is that the nullity of at least one of the individual desirabilities leads to the nullity of the global desirability. The highest D value is obtained under conditions where the combination of the different responses is globally optimal.

In order to use the global desirability function, the problem could be formulated as:

$$Max\ D = \left[\prod d_i^{wi}\right]^{1/\sum wi} \tag{17}$$

where D represents overall desirability, d_i is the individual desirability for the ith response and wi is the weight of the ith response.

The traditional desirability function method proposed by Derringer is employed to calculate individual desirability for each response. We use Y_i, Y_c, $Y_{i,\min}$, $Y_{i,\max}$ and w_i to denote, respectively, the predicted value, the target value, the lowest acceptable value, the highest acceptable value and the weight of desirability function of the ith output response.

To look for a maximum value for a response, the individual desirability is calculated as:

$$d_i = \begin{cases} 0 & \Leftrightarrow \quad Y_i \le Y_{i,\min} \\ \left[\dfrac{Y_i - Y_{i,\min}}{Y_{i,\max} - Y_{i,\min}}\right]^{w_i} & \Leftrightarrow \quad Y_{i,\min} \le Y_i \le Y_{i,\max} \\ 1 & \Leftrightarrow \quad Y_i \ge Y_{i,\max} \end{cases} \tag{18}$$

To look for a minimum value for a response, the individual desirability is calculated as:

$$d_i = \begin{cases} 1 & \Leftrightarrow \quad Y_i \le Y_{i,\min} \\ \left[\dfrac{Y_i - Y_{i,\max}}{Y_{i,\min} - Y_{i,\max}}\right]^{w_i} & \Leftrightarrow \quad Y_{i,\min} \le Y_i \le Y_{i,\max} \\ 0 & \Leftrightarrow \quad Y_i \ge Y_{i,\max} \end{cases} \tag{19}$$

In the case where we wish to have a target value of a response, the desirability function is calculated as:

$$d_i = \begin{cases} 0 & \Leftrightarrow \quad Y_i \le Y_{i,\min}, Y_i \ge Y_{i,\max} \\ \left[\dfrac{Y_i - Y_{i,\min}}{Y_c - Y_{i,\min}}\right]^{r_i} & \Leftrightarrow \quad Y_{i,\min} \le Y_i \le Y_c \\ \left[\dfrac{Y_i - Y_{i,\max}}{Y_c - Y_{i,\max}}\right]^{r_i} & \Leftrightarrow \quad Y_c \le Y_i \le Y_{i,\max} \\ 1 & \Leftrightarrow \quad Y_i = Y_c \end{cases} \tag{20}$$

To maximize the overall desirability function, Nemrodw software uses the simulated annealing method. This method is a general probabilistic algorithm for optimization problems [21] [22]. It uses a process of searching for a global optimal solution in the solution space that is analogous to the physical process of annealing.

3. Optimization of the OMUX Resonator Using Central Composite Designs

3.1. Reference Structure

In a transmission system, a multichannel output multiplexer filter (OMUX) is behind the power amplifier module. Its role is to select the channel narrow-band signal and thus, eliminate the frequency noise created by amplifiers. This filter is characterized by low insertion losses and high quality factor due to its location between the power amplifier and antenna. The selectivity has to be high because the different channels to be multiplexed can have very similar bands. An OMUX filter is made with a dual-mode cylindrical cavity and filled with air [7] [23].

The system studied consists of a parallelepiped-shaped resonator (**Figure 2**) truncated at the 4 corners and short-circuited in a cylindrical cavity. It has four contacts with the metal walls, which ensure its maintenance.

The structure was analyzed by the finite element method (FEM) [24]; FEM is a popular technique for analyzing microwave components [25] since both planar and waveguide structures (including antennas) can be treated. Modeling a microwave component with FEM requires discretizing the structure into small mesh elements before solving.

The dimensions of reference are its diameter denoted by Dc = 39.86 mm and its height denoted by Hc = 28 mm. The resonator thickness E is equal to 3 mm.

The relative permittivity of the dielectric material is $\varepsilon_r = 12.6$ with a loss tangent $\tan\delta = 5.5 \times 10^{-5}$, the metallic conductivity σ of the cavity is equal to 4.76×10^7 S·m^{-1}.

The electromagnetic simulation given in **Figure 3** shows that the filter presents two excited modes (at the frequencies F_0 and F_2) and a non-excited mode at the frequency F_1 (between F_0 and F_2).

The quality factor Q_0 of the resonator is equal to 10,145. The aim of the optimization of this resonator is to hold off the two frequencies F_1 and F_2 ($F_1 \geq 4.5$ GHz and $F_2 \geq 6$ GHz) from the fundamental frequency F_0 and have the largest value of the quality factor Q_0.

3.2. Optimization of the Cavity Dimensions

In order to optimize the characteristics of resonator, a first study was done according to the parameters describing the cylindrical cavity (**Figure 2**). The two factors describing the cavity are its height Hc (which varies between 21 and 35 mm) and its diameter Dc (which varies between 30 and 50 mm). The thickness of the resonator E is not involved in the optimization; it has been calculated to have a frequency of the first excited mode F_0 always equal to 4 GHz.

$$\hat{Y} = b_0 + b_1 X_1 + b_2 X_2 + b_{11} X_1^2 + b_{22} X_2^2 + b_{12} X_1 X_2 + \varepsilon \tag{21}$$

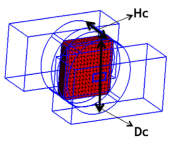

Figure 2. OMUX resonator: reference structure.

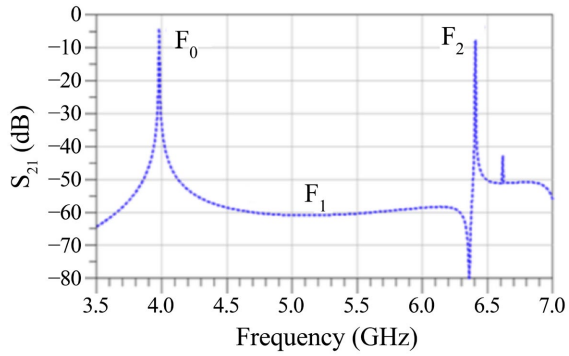

Figure 3. Simulated response (S_{21} scattering parameter).

We are interested in this part of the design of experiments in which factors have many levels; there is no difficulty in changing the levels of these two factors, so we chose a CCC design that allows five levels per factor. In our case, the number of input factor is equal to two, resulting in 9 experiments to be performed. The model used is a polynomial of degree 2 written as follow.

The design of experiments has been constructed from the experiment matrix containing the coded values of input factors. In this study, the experiment is a simulation using the software EMXD [26] that is based on FEM. The design of experiments contains 9 lines; the thickness of the resonator is calculated for each line of the design, which gives a frequency of the first excited mode F_0 equal to 4 GHz. The value of α in our case is 1.4; the experimental range and levels of independent variables are given in **Table 3**.

After building the experimental design and performing the simulations, the next step is to validate the mathematical models for each response. The statistical software 'NemrodW) [27] has been used to study the regression analysis of experimental data and to draw the response surface plot. The standard analysis of variance (ANOVA) and model coefficients for the response F_1 are presented in **Table 4**. The ANOVA confirms adequacy of the quadratic model since its Prob (F_c) value is equal to 0.955.

The fit of the model was checked by the determination coefficient (R^2). For response F_1, the value of R^2 is 0.98, thus ensuring a satisfactory adjustment of the model to the experimental data and indicating that approximately 98% of the variability in the dependent variable (response F_1) could be explained by this model. The value of the adjusted determination coefficient is 0.946, attesting once more, the reliability of the model.

The ANOVA tables are given for each response; the Prob (F_c) values and the R^2, R^2_{adj} coefficients are given in **Table 5**.

Table 3. Experimental variables and their coded levels.

Factor	−1.41	−1	0	1	1.41	Coded values
Dc (mm)	25.9	30	40	50	54.1	Real values
Hc (mm)	18.1	21	28	35	37.9	

Table 4. Analysis of variance (ANOVA) table for the response F_1.

Source	Sum of squares	Degree of freedom	Mean square	F_c
Regression	1.9637	5	0.3927	29.1467
Error	0.0404	3	0.0135	
Total	2.0041	8		

Table 5. Statistical parameters obtained from the ANOVA for the models for all responses.

Coefficients	Responses		
	F_1	F_2	Q_0
R^2	0.98	0.997	0.998
R^2_{adj}	0.946	0.992	0.995
Prob (F_c)	0.96%	0.06%	0.03%

It could be seen from **Table 5** that the mathematical models for all responses are validated: Prob (F_c) < 5% and R^2, R^2_{adj} are close to 1.

The experimental domain is defined by the variation of two factors; graphical analysis can help us study their effects on each response. The effects of input factors Dc and Hc on all responses are given by three-dimensional graphics called response surfaces (**Figure 4**). The horizontal plane of the figure represents the range of variation of the two factors Dc and Hc; the vertical axis materializes the variation of responses.

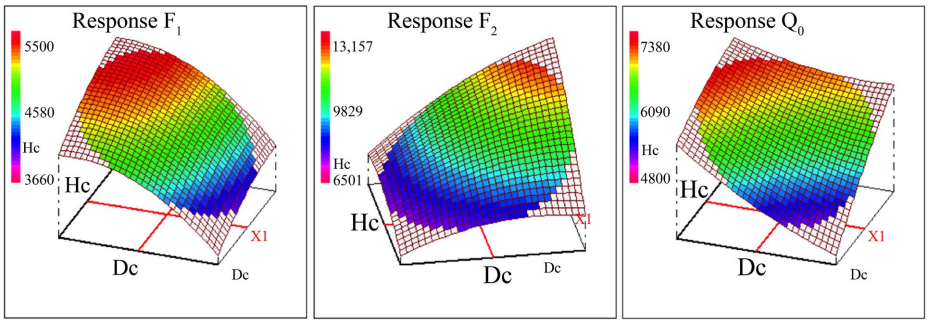

Figure 4. Response surfaces for F_1, F_2 and Q_0.

By observing these figures, we see that: the frequency of the first excited mode F_1 increases when Hc increases and Dc decreases; the frequency of the second excited mode F_2 increases when Hc increases and Dc decreases; the quality factor Q_0 increases by increasing Dc and Hc.

The good quality of the models could be seen from the model adequacy graph. This graph is used to compare the simulated responses and the responses estimated by the model. The measured (experimental) responses are placed on the x-axis and the estimated (model-calculated) responses on the y-axis. If the scatterplot is aligned on the equation line $y = x$, the descriptive quality of the model is

excellent (we consider that the values calculated by the model are very close to the measured values). The adequacy graph for each response is given in Figure 5 and shows a very good quality of the mathematical model; indeed, the experimental points, are placed perfectly on the line $y = x$.

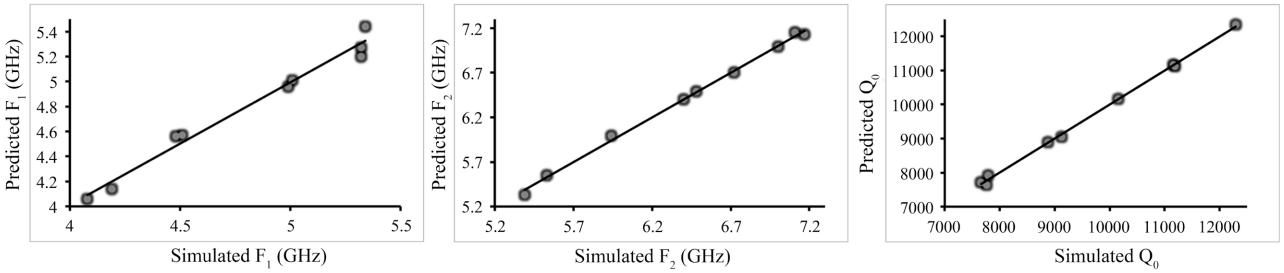

Figure 5. Predicted based on the model versus actual values of the three responses.

3.3. Results and Discussion

The search for a multi-criteria optimum consists of finding the level of factors that maximizes the value of the global desirability function. In our case, we are looking for a maximum value for all the responses.

Figure 6 shows the individual desirability functions $d1$, $d2$ and $d3$ of the responses F_1, F_2 and Q_0. A value of 4.5 GHz has been specified as the minimum accepted value for the response F_1. We are also looking for a value of F_2 higher than 6 GHz and a maximum value of the answer Q_0 (above 10,000). The same weight is assigned to the three responses, which gives an overall desirability function:

$$D = \left(d1 \times d2 \times d3\right)^{1/3} \tag{22}$$

A high percentage of individual desirability for both responses F_1 ($d1$ = 100%) and F_2 ($d2$ = 100%) is obtained. The values of these two responses calculated by the model are 4.57 GHz for F_1 and 6.7 GHz for F_2.

The value of the individual desirability function for the response Q_0 is 11.7%. This value is considered low since the value searched for Q_0 is 30,000 and the model finds 12,341. All these values of the individual desirability functions lead to an overall desirability of 48.91%.

Optimization results obtained by the CCC design are given in Table 6. In this table, the optimal values of the input factors, as well as the calculated responses and the simulated responses, are given. The good quality of models could be seen from the insignificant difference between calculated and simulated responses. A quality factor of 12,291 has been found, leading to an improvement of 21.1% compared to the reference quality factor (10,145). Frequency isolation is well ensured since the frequency F_1 is greater than 4.5 GHz and the frequency F_2 is greater than 6 GHz.

The optimal value found using a CCC design is given in Figure 7; it can be seen that this value is located at the limit of the experimental region. These results lead

us to create a new CCF design with only 6 new experiments instead of 9, as shown in Figure 7.

After performing the simulations, the mathematical model has been validated and a multicriteria optimization has been conducted leading to results in Table 7.

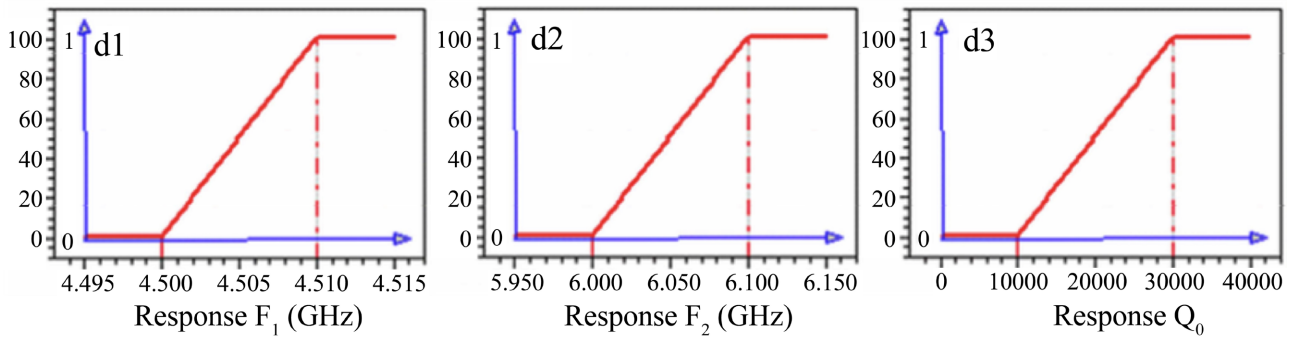

Figure 6. Individual desirability functions for F_1, F_2 and Q_0.

Table 6. Optimization results obtained using CCC design.

CCC design	Optimal values		Responses		
	Dc	Hc	F_1	F_2	Q_0
Model	50	35	4.57	6.7	12,341
Simulation	50	35	4.48	6.72	12,291

The good quality of models could be seen from the insignificant difference between calculated and simulated responses. A quality factor of 12,680 has been found, leading to an improvement of 24.9% compared to the reference quality factor (10,145). Frequency isolation is well ensured since the frequency F_1 is greater than 4.5 GHz and the frequency F_2 is greater than 6 GHz.

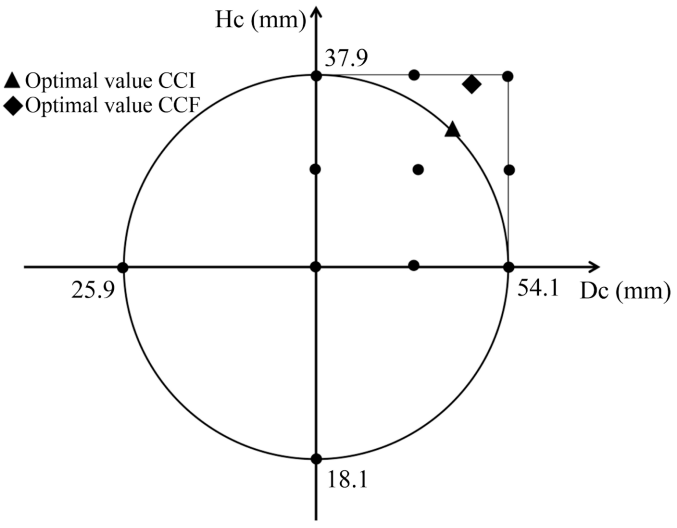

Figure 7. Optimal values found using CCI and CCF designs.

Table 7. Optimization results obtained using CCF design.

CCF design	Optimal values		Responses		
	Dc	Hc	F_1	F_2	Q_0
Model	50	37.5	4.54	6.69	12,671
Simulation	50	37.5	4.57	6.91	12,680

4. Optimization of the Resonator Using Level Set Method and RSM

In the previous section, RSM was used to optimize the dimensions of the cylindrical cavity. Indeed, the application of RSM does not allow changing the topology or the shape of the resonator inside the cylindrical cavity. There are several shape optimization methods that allow optimizing the shape and topology of the component [28]-[31], such as the topology gradient (TG) method and the Level Set (LS) method. In this section, the LS method is used to optimize the form of the resonator and then the RSM is applied by introducing new parameters (input factors) to the experimental design. The aim of this study is to maximize the quality factor compared to the reference value while ensuring frequency isolation.

Level-set (LS) method [32] has recently received a growing attention for shape reconstruction problems. The main idea of LS methods lies in representing the evolving interface of the object (curve or surface) as the zero-level of a higher-order function. A LS method is a versatile and simple method for tracking the motion of an interface (in two or three dimensions) estimating a gradient based on the shape derivative with respect to given constraints.

The variables in the level set method are defined by the outline of the resonator. The outline almost approaches the borders of the mesh elements. A more rigorous treatment of the level-set method can be found in [33], which provided the background for this section. The optimization by the level set method is used to minimize a cost function.

The optimized shape of the resonator by the level set method shown in **Figure 8(a)**, focuses the dielectric material in the center of the cavity to limit losses. More details about the application of LS method can be found in [32]. The optimization by the level set method leads to a quality factor of 12,325 providing an improvement of 21.4%. The form obtained by the level set method has been approximated by a dielectric cylinder of the same material to reduce the number of geometric parameters as shown in **Figure 8(b)**.

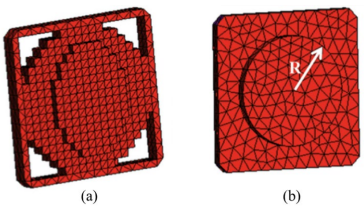

Figure 8. Optimized shape by Level Set method (a) and approached shape to use RSM method (b).

4.1. Application of a CCF Design to Optimize the Resonator and the Cavity Dimensions

In this section, the RSM is used, taking into account three factors: the dimensions of the cavity (Dc and Hc) and the radius (R) of the plate. The design of experiments used in this section is CCF, in this case, the field is cubic which gives the possibility to find optima which is next to the extreme values of the factors. For $k = 3$ factors, the number of experiments to be carried out is 15 and the corresponding experimental design is given in Table 8.

It has been shown previously that the quality factor increases with the cavity dimensions Dc and Hc. We have therefore reduced the experimental ranges of these two factors where the quality factor is at its maximum. The new experimental ranges of the input factors are: Dc between 44 and 48 mm, Hc between 28 and 36 mm and R between 8 and 14.8 mm.

Table 8. Experimental design and simulated responses.

Run	Input factors			Responses		
	Dc (mm)	Hc (mm)	R (mm)	F_1 (GHz)	F_2 (GHz)	Q_0
1	40	28	8	3.51	4.49	12,640
2	48	28	8	3.95	5.18	12,615
3	40	36	8	5.18	6.88	12,688
4	48	36	8	4.65	6.84	12,659
5	40	28	14.8	4.71	6.03	11,200
6	48	28	14.8	4.52	6.06	11,845
7	40	36	14.8	5.29	6.71	11,776
8	48	36	14.8	4.66	6.83	12,483
9	40	32	11.4	4.99	6.51	12,153
10	48	32	11.4	4.60	6.58	12,388
11	44	28	11.4	4.69	6.13	12,186
12	44	36	11.4	5.03	7.52	12,445
13	44	32	8	4.78	6.89	12,761
14	44	32	14.8	4.99	6.44	12,004
15	44	32	11.4	4.96	6.58	12,334

Table 9. Statistical parameters obtained from the ANOVA for the models for all responses.

Coefficients	Responses		
	F_1	F_2	Q_0
R^2	0.98	0.997	0.998
R^2_{adj}	0.946	0.992	0.995
R^2_{pred}	0.361	0.215	0.97
Prob (F_c)	0.96%	0.06%	0.03%

The statistical parameter obtained from ANOVA was shown in Table 9.

It can be seen that the model of the response Q_0 is of high quality since the values of R^2, R^2_{adj}, and R^2_{pred} are close to 1. On the other hand, the predictive quality of the mathematical models of the responses F_1 and F_2 is poor (R^2_{pred} = 0.361 for the response F_1 and 0.215 for F_2). These results will be verified by estimating the difference between the calculated and simulated responses on the $k+1$ test points proposed by the Nemrodw software. In this case, 4 test points are necessary to validate the model at any point in the experimental domain. The calculated responses on these points as well as the values obtained by simulations are given in Figure 9.

The bad predictive quality of the models for the responses F_1 and F_2 could be clearly seen in Figure 9; indeed, the experimental test points are not closely distributed around the line $y = x$.

In the present case, we are mainly interested in the quality of the model of the Q_0 response. Indeed, according to the experimental design (Table 8), frequency isolation could be easily ensured. The goal is then to find the maximum of the quality factor Q_0.

4.2. Multicriteria Optimization Results

Multi-criteria optimization results are given in **Table 10**. The best solution has been found for a radius R = 8 mm, a diameter Dc of 43.6 mm and a height Hc of 32.7 mm. The results obtained can show the relevance of the coupling the level set and design of experiments method. Indeed, although the independent use of each of these two methods improves the quality factor (respectively 21.48% and 25.36% compared to the reference value), their coupling as described in this work leads to an improvement of 25.77% as shown in Figure 10. In addition, we have demonstrated a solution whose volume is 34.5% lower than that identified by using only designs of experiments method, and therefore more economical to manufacture.

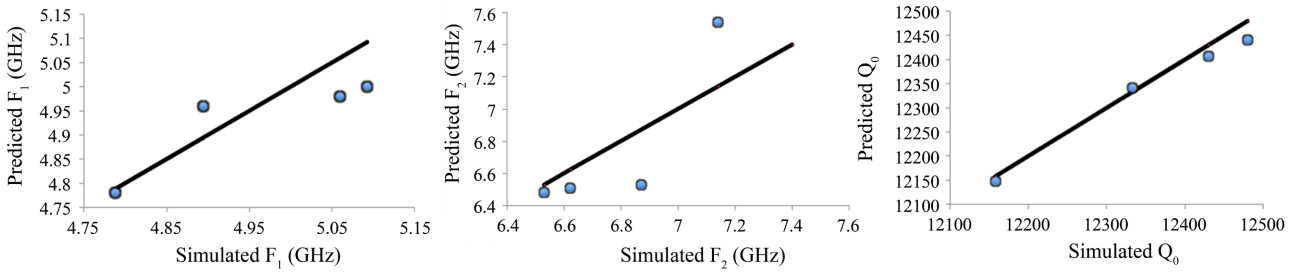

Figure 9. Predicted based on the model versus actual values for F_1, F_2 and Q_0 on test points.

Table 10. Optimization results.

CCF design	Optimal values			Responses		
	Dc	Hc	R	F_1	F_2	Q_0
Model	43.6	32.7	8	4.77	6.58	12,785
Simulation	43.6	32.7	8	4.87	6.68	12,760

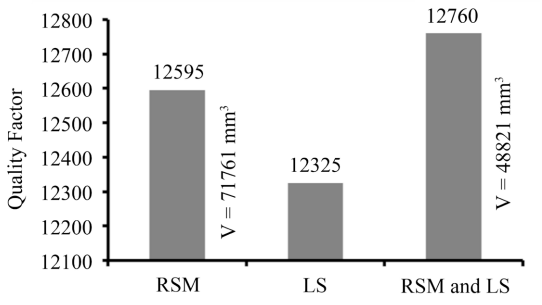

Figure 10. Quality factor optimization.

4.3. Experimental Validation

For validating the optimization techniques, the initial and optimized resonators have been fabricated using a stereolithography process [34]; the photograph of the fabricated resonators is given in **Figure 11**.

The left part of **Figure 12** shows the simulated responses of both the initial and optimized resonators, while the right part presents the measured responses of the fabricated resonators. It can be observed that the optimized resonator operates exactly at 4 GHz. The isolation frequency is well ensured, and the measured quality factor is 12,760, resulting in an improvement of 25.77% compared to the reference structure.

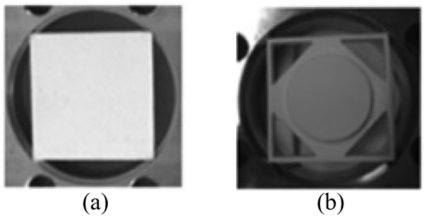

Figure 11. Initial (a) and optimized (b) resonators.

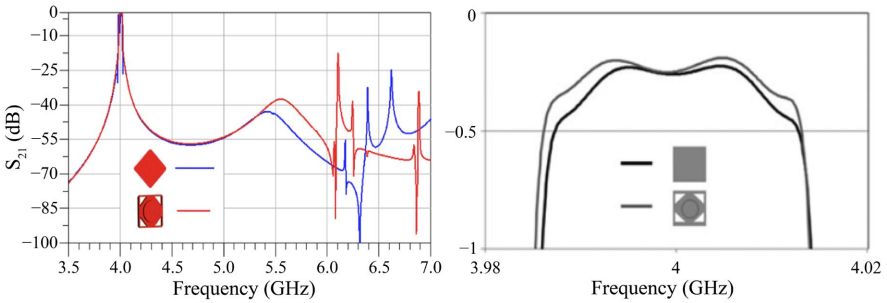

Figure 12. Measured response for the initial and optimized resonators.

5. Conclusion

Different shape optimization methods are available nowadays and can be applied to the design of microwave devices. These approaches are often local, based on the calculation of a gradient, and allow, to a certain extent, to reach an unknown optimal solution. In this study, RSM has been used to optimize OMUX resonator

where central composite designs are used in both spherical and cubic domains. RSM was first used to optimize the cylindrical cavity containing the resonator; the application of this method resulted in a 25.3% improvement in the quality factor compared to the reference value. LS method was then applied to optimize the resonator in the cylindrical cavity. The application of this method concentrates the material in the center of the resonator and makes it possible to apply RSM to optimize the cylindrical cavity and the resonator together. The results obtained show the relevance of coupling different optimization methods, such as the LS method and RSM. Indeed, although the independent use of each of these two methods has improved the quality factor respectively by 21.48% and 25.36% compared to the reference value, their coupling as described in this work leads to an improvement of 25.77%. In addition, the optimized structure presents a volume 34.5% lower than that identified by using experimental designs only, and therefore more economical to manufacture.

Conflicts of Interest

The authors declare no conflicts of interest regarding the publication of this paper.

References

[1] Box, G.E.P. and Wilson, K.B. (1951) On the Experimental Attainment of Optimum Conditions. *Journal of the Royal Statistical Society Series B: Statistical Methodology*, **13**, 1-38. https://doi.org/10.1111/j.2517-6161.1951.tb00067.x

[2] Muzeau, J.P. and Lemaire, M. (1997) Reliability Analysis with Implicit Formulations. In: Soares, C.G., Ed., *Probabilistic Methods for Structural Design*, Springer, 141-160. https://doi.org/10.1007/978-94-011-5614-1_7

[3] Stevens, W.L. (1951) Asymptotic Regression. *Biometrics*, **7**, 247-267. https://doi.org/10.2307/3001809

[4] Wishart, J. (1939) Statistical Treatment of Animal Experiment. *Journal of the Royal Statistical Society*, **6**, 1-22. https://doi.org/10.2307/2983620

[5] Osborne, D.M., Armacost, R.L. and Pet-Edwards, J. (1997) State of the Art in Multiple Response Surface Methodology. 1997 *IEEE International Conference on Systems, Man, and Cybernetics. Computational Cybernetics and Simulation*, Orlando, 12-15 October 1997, 3833-3838. https://doi.org/10.1109/icsmc.1997.633268

[6] Gao, X.K., Low, T.S., Liu, Z.J. and Chen, S.X. (2002) Robust Design for Torque Optimization Using Response Surface Methodology. *IEEE Transactions on Magnetics*, **38**, 1141-1144. https://doi.org/10.1109/20.996292

[7] Atia, A.E. and Williams, A.E. (1972) Narrow-Bandpass Waveguide Filters. *IEEE Transactions on Microwave Theory and Techniques*, **20**, 258-265. https://doi.org/10.1109/tmtt.1972.1127732

[8] Anderson, C.M., Montgomery, C.D. and Myers, H.R. (2016) Response Surfaces Methodology. In: *Process and Product Optimization Using Designed Experiments*, 4th Edition, Wiley, 111, 297-320.

[9] Zhang, Z. and Xiaofeng, B. (2009). Comparison about the Three Central Composite Designs with Simulation. 2009 *International Conference on Advanced Computer Control*, Singapore, 22-24 January 2009, 163-167. https://doi.org/10.1109/icacc.2009.48

[10] Chollom, M.N., Rathilal, S., Swalaha, F.M., Bakare, B.F. and Tetteh, E.K. (2019) Comparison of Response Surface Methods for the Optimization of an Upflow Anaerobic Sludge Blanket for the Treatment of Slaughterhouse Wastewater. *Environmental Engineering Research*, **25**, 114-122. https://doi.org/10.4491/eer.2018.366

[11] Lundstedt, T., Seifert, E., Abramo, L., Thelin, B., Nyström, Å., Pettersen, J., *et al.* (1998) Experimental Design and Optimization. *Chemometrics and Intelligent Laboratory Systems*, **42**, 3-40. https://doi.org/10.1016/s0169-7439(98)00065-3

[12] Box, G.E.P. and Hunter, J.S. (1957) Multi-Factor Experimental Designs for Exploring Response Surfaces. *The Annals of Mathematical Statistics*, **28**, 195-241. https://doi.org/10.1214/aoms/1177707047

[13] Khoder, K. (2011) Optimisation de Composants Hyperfrequences par la Technique des Plans a Surface des Reponses. PhD Thesis, University of Limoges. https://doi.org/10.6084/m9.figshare.12086298

[14] Ying, L.H., Pukelsheim, F. and Draper, N.R. (1995) Slope Rotatability over All Directions Designs. *Journal of Applied Statistics*, **22**, 331-341. https://doi.org/10.1080/757584723

[15] Kasina, M.M., Joseph, K. and John, M. (2020) Application of Central Composite Design to Optimize Spawns Propagation. *Open Journal of Optimization*, **9**, 47-70. https://doi.org/10.4236/ojop.2020.93005

[16] Draper, N. and Smith, H. (1981) Applied Regression Analysis. Wiley Series in Probability and Statistics, Wiley.

[17] Heiberger, R.M. (1981) The Specification of Experimental Designs to ANOVA Programs. *The American Statistician*, **35**, 98-104. https://doi.org/10.1080/00031305.1981.10479316

[18] Harrington, E. (1965) The Desirability Function. *Industrial Quality Control*, **21**, 494-498.

[19] Derringer, G. and Suich, R. (1980) Simultaneous Optimization of Several Response Variables. *Journal of Quality Technology*, **12**, 214-219. https://doi.org/10.1080/00224065.1980.11980968

[20] He, Z. and Zhu, P.F. (2008) A Note on Multi-Response Robust Parameter Optimization Based on RSM. 2008 4*th IEEE International Conference on Management of Innovation and Technology*, Bangkok, 21-24 September 2008, 1120-1123. https://doi.org/10.1109/icmit.2008.4654526

[21] Liu, J.S., Liang, F. and Wong, W.H. (2000) The Multiple-Try Method and Local Optimization in Metropolis Sampling. *Journal of the American Statistical Association*, **95**, 121-134. https://doi.org/10.1080/01621459.2000.10473908

[22] Gallo, C. and Capozzi, V. (2019) A Simulated Annealing Algorithm for Scheduling Problems. *Journal of Applied Mathematics and Physics*, **7**, 2579-2594. https://doi.org/10.4236/jamp.2019.711176

[23] Williams, A.E. (1970) A Four-Cavity Elliptic Waveguide Filter. *IEEE Transactions on MIT*, **18**, 1109-1114. https://doi.org/10.1109/gmtt.1970.1122775

[24] Bila, S., Baillargeat, D., Aubourg, M., Verdeyme, S. and Guillon, P. (2000) A Full Electromagnetic CAD Tool for Microwave Devices Using a Finite Element Method and Neural Networks. *International Journal of Numerical Modelling: Electronic Networks, Devices and Fields*, **13**, 167-180. https://doi.org/10.1002/(sici)1099-1204(200003/06)13:2/3<167::aid-

jnm354>3.0.co;2-w

[25] Webb, J.P. and Akel, H. (2000) Design Sensitivities for Scattering-Matrix Calculation with Tetrahedral Edge Elements. *IEEE Transactions on Magnetics*, **36**, 1043-1046. https://doi.org/10.1109/20.877620

[26] Aubourg, M., Guillon, P., Verdeyme, S. and Madrangeas, V. (1994) Modeling Microwave Boxed Structures by 2D and 3D Finite Element Method. *International Journal for Computation and Mathematics in Electrical and Electronic Engineering*, **13**, 335-340.

[27] Mathieu, D., Nony, J. and Phan-Tan-Luu, R. (2000) Nemrod-W Software, Marseille. https://www.Nemrodw.com

[28] Sethian, J.A. and Wiegmann, A. (2000) Structural Boundary Design via Level Set and Immersed Interface Methods. *Journal of Computational Physics*, **163**, 489-528. https://doi.org/10.1006/jcph.2000.6581

[29] Jackowska-Strumillo, L., Sokolowski, J. and Zochowski, A. (1999) The Topological Derivative Method in Shape Optimization. *Proceedings of the* 38*th IEEE Conference on Decision and Control*, Vol. 1, 674-679. https://doi.org/10.1109/cdc.1999.832864

[30] Kiziltas, G., Psychoudakis, D., Volakis, J.L. and Kikuchi, N. (2003) Topology Design Optimization of Dielectric Substrates for Bandwidth Improvement of a Patch Antenna. *IEEE Transactions on Antennas and Propagation*, **51**, 2732-2743. https://doi.org/10.1109/tap.2003.817539

[31] Allaire, G., Jouve, F. and Maillot, H. (2004) Topology Optimization for Minimum Stress Design with the Homogenization Method. *Structural and Multidisciplinary Optimization*, **28**, 87-98. https://doi.org/10.1007/s00158-004-0442-8

[32] Allaire, G., De Gournay, F., Jouve, F. and Toader, A.M. (2005) Structural Optimization Using Topological and Shape Sensitivity via a Level Set Method. *Control Cybernetics*, **34**, 59-81.

[33] Mahdi, N., Bila, S., Verdeyme, S., Aubourg, M., Khoder, K., Bessaudou, A., *et al.* (2013) A Shape Optimization Library for the Design of Microwave Components. *International Journal of Microwave and Wireless Technologies*, **6**, 31-37. https://doi.org/10.1017/s1759078713000950

[34] Duterte, C., Delhote, N., Baillargeat, D., Verdeyme, S., Abouliatim, Y. and Chartier, T. (2007) 3D Ceramic Microstereolihography Applied to Sub-Millimeter Devices Manufacturing. 37*th European Microwave Conference*, Munich, 8-12 October 2007, 814-817. https://doi.org/10.1109/eumc.2007.4405317